Honda Research Institute EU
Honda Research Institute Europe GmbH
https://www.honda-ri.de/

State-based Representation for Structural Topology Optimization and Application to Crashworthiness

Nikola Aulig, Markus Olhofer

2016

Preprint:

This is an accepted article published in Proceedings of: IEEE Congress on Evolutionary Computation. The final authenticated version is available online at: https://doi.org/[DOI not available]

State-based Representation for Structural Topology Optimization and Application to Crashworthiness

Nikola Aulig
Honda Research Institute Europe GmbH
Carl-Legien-Straße 30
63073 Offenbach/Main, Germany
Email: nikola.aulig@honda-ri.de

Markus Olhofer
Honda Research Institute Europe GmbH
Carl-Legien-Straße 30
63073 Offenbach/Main, Germany
Email: markus.olhofer@honda-ri.de

***Abstract*—Structural topology optimization addresses the problem of providing designers and engineers with concepts of mechanical structures. Evolutionary optimization algorithms are suitable for practical domains, such as crashworthiness problems, that are characterized by strong non-linearities and black box simulations. However, due to the high computational cost of the structural analysis, their application requires a representation, that avoids excessive computational cost. In this work, we propose an algorithm based on two main concepts. Firstly, we propose a novel, adaptive and low dimensional representation of the discretized structural design space. It is based on a clustering of design space elements, which show similar Local State Features such as energies or displacements and is dynamically updated during the optimization. Secondly, instead of directly modifying the structure, an evolutionary optimization provides update signals, that determine the decrease or increase of the amount of material for each of the distinct clusters of elements. The de-randomized Evolution Strategy with Covariance Matrix Adaptation is used to optimize the vector of update signals, hence optimizing the change of the material distribution. The feasibility of the method is at first demonstrated on a compliance minimization reference problem and subsequently applied to a problem from the field of crashworthiness topology optimization, for which standard gradient-based methods are not feasible. The novel method achieves remarkably better performance, when compared to a baseline obtained by a uniform energy heuristics for crashworthiness topology optimization.**

I. Introduction

Topology optimization of mechanical structures is an important industrial problem, that addresses the task of finding concept structures early in the design process. In contrast to sizing and shape optimizations, the target is to find a starting concept for the basic geometric layout of the design. In this paper, we introduce a novel representation and evolutionary optimization approach for topology optimization. It targets practical problems, that are characterized by strong non-linearities and black box simulations, for which classical gradient-based methods are not suitable.

Typically a defined design space serves as starting point for a topology optimization. Boundary conditions such as loads (e.g. forces) and supports (i.e. locations where the structure is fixed) are applied. An example can be seen in the experiments section in Fig. 5a). The optimization target is to find the distribution of material and void within this design space.

One of the most popular standard approaches are density-based topology optimization methods [1], [2]. These operate on a mesh representation. The performance evaluation of a structure within the design space requires its discretization in a mesh of finite elements, hence an obvious approach is to assign a variable for each element in the mesh. The problem can be formulated as:

$$\begin{aligned} &\min_{\boldsymbol{\rho}} \; f(\boldsymbol{\rho}, \mathbf{u}) \\ &\text{s.t.} : G_0 = V(\boldsymbol{\rho}) - V_0 \leq 0, \\ &\qquad 0 \leq \rho_{\min} \leq \rho_i \leq 1, \; i = 1, \ldots, N \;\; , \end{aligned} \tag{1}$$

where $f(\boldsymbol{\rho})$ is the objective function, $\boldsymbol{\rho}$ is the vector of design variables, in which each component ρ_i corresponds to the material density in element i, $i = 1 \ldots N$, and $\rho_{\min}$ is a minimum density. The minimum density is slightly larger than zero in order to avoid numerical instabilities. A volume constraint G_0 on the volume $V(\boldsymbol{\rho}) = \sum_{i=1}^{N} \rho_i v_i$ of the structure, is defined, where v_i is the element volume and V_0 is the design space volume. The state vector $\mathbf{u}$ is obtained from solving the governing equation of the problem.

A key idea is the interpolation of material properties that relaxes the originally discrete problem into its continuous form in (1), known as Solid Isotropic Material with Penalization (SIMP) [3]:

$$E_i(\rho_i) = \rho_i^p E_0 \;\; , \tag{2}$$

where E_0 is a material property, for instance the Young's modulus.

The relaxation enhances the use of gradient-based optimization. An example for an optimization result is given in Fig. 5b) when maximizing the stiffness (compare Sec. IV-A). Note that a discrete design can be easily obtained by thresholding of the densities.

The existing gradient-based methods can efficiently handle vast design spaces with up to millions of variables. However, these methods can only be applied to objective functions for which gradients are available and suitable. This limitation motivates the search for alternative methods based on evolutionary algorithms.

The practical problem addressed in this paper is crashworthiness topology optimization, which is relevant in the design process of vehicles with regard to passive safety requirements.

Crash simulation and optimization is a challenging task in design optimization, that requires non-linear modeling, e.g. with respect to displacements, materials and contacts. This can result in multi-modal, noisy and discontinuous objective functions. Therefore, the standard gradient-based topology optimization methods can only be applied for considerably simplified problems and are currently replaced by specialized heuristic methods [4], [5].

Evolutionary optimization algorithms can be useful for this class of objective functions. However, finite element simulations in general, and crash simulations in particular are computationally expensive and can take from minutes up to days to run, depending on the complexity of the task and available parallel computing power. Therefore, an important issue is to find an appropriate representation of the structure. An overview on Evolutionary Computation (EC) approaches can be found in literature, with a focus on structural design [6] and more recently on representations [7].

Genetic algorithms that operate on a grid representation [8], [9] (where the search dimensionality increases with the resolution) assign a variable to each element, and therefore are mostly suitable for problems with coarse mesh resolutions, a fact that is criticized in [10]. Alternatives are geometric representations that describe the structure by a set of parameterized shape primitives [11]–[13], however involving assumptions on the form and complexity of the optimal solution. Indirect representations [14]–[16] use a, sometimes quite complex, generative process to construct the structure.

The basis of the efficient gradient-based optimization approaches is formed by usage of the state information, obtained from the structural analysis. Despite the existence of many elaborate EC approaches, the potential value of using this information in the optimization is commonly neglected. An exception is [17], [18], in which a hybrid neuro-evolutionary topology optimization approach is proposed. Concretely, local information within the structure, such as displacements and stain energies, is processed by an artificial neural network model that determines an update signal to modify the structure. The neural network model parameters are optimized by an evolutionary optimization. In this paper we extend this approach by using state information as means for an indirect representation of the design space, especially taking into account that areas with similar local information are likely to have a similar effect on the objective function.

Section II introduces the novel representation. The corresponding optimization method is introduced in Sec. III. The method is validated on the minimum compliance reference problem in Sec. IV-A, followed by its application to a problem from the field of crashworthiness topology optimization in Sec. IV-B. The paper is concluded in Sec. V.

II. State-based Representation

This section introduces a state-based representation to address the problem defined in (1). Before formally introducing the representation, we start the section by visualizations of the physical information that is used by the method.

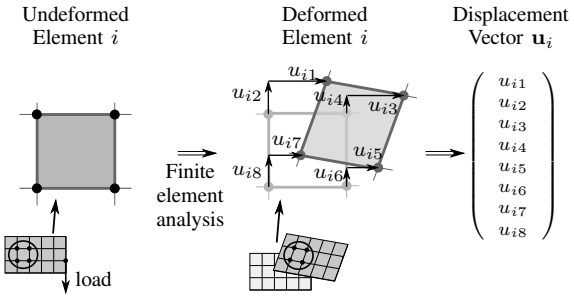

Fig. 1. Local state features example: Displacements of element nodes when a finite element analysis is performed.

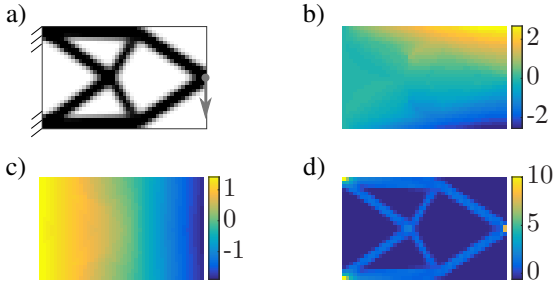

Fig. 2. Example for: a) Density distribution of cantilever structure subject to static load; Resulting normalized Local State Features: b) first nodal displacement component (horizontal), c) second nodal displacement component (vertical), d) strain energy.

Figure 1 presents the state of a two-dimensional square finite element which is defined by four nodes. It is shown in undeformed and a deformed state. The deformed state is the result of applying a load and performing a finite element analysis. The state is "local" with respect to the element considered, it is composed of the local nodal displacements, i.e. the variables which are solved for by a finite element solver. From displacements also other physical indicators such as stresses or energies can be computed. Figure 2 illustrates the state of a two-dimensional cantilever structure in a design space subject to a static load. Different types of state information are color coded throughout the design space.

These physical features are obtained from the structural state and are local with respect to the element, hence they can be termed Local State Features (LSF) as in [17]. Depending on the state, each element i relates to a point in LSF space by its LSF vector $\mathbf{s}_i \in \mathbb{R}^J$, with the number of LSF J. The actual LSFs depend on the problem and the choice of the user. This results in a data set $\mathcal{V} = \{\mathbf{s}_1, \ldots, \mathbf{s}_N\}$ and is illustrated in Fig. 3a) and b) for a two-dimensional LSF space.

In gradient-based approaches the partial derivatives (also referred to as "sensitivities") are computed based on these LSF, i.e. $\frac{\partial f}{\partial \rho_i} = \frac{\partial f}{\partial \rho_i}(\mathbf{s}_i)$. For problems such as the minimum compliance problem addressed below in Sec. IV-A, analysis reveals that all elements having the same state, also have the same sensitivity value (for the sensitivity analysis the reader is referred to [1]). This motivates a state-based representation by grouping elements that are assumed to have similar influence

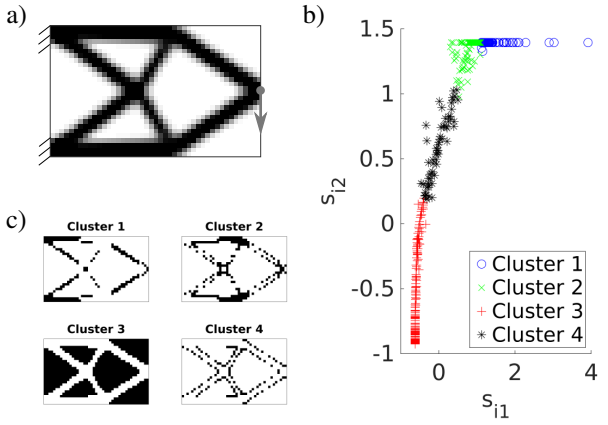

Fig. 3. Example for: a) Density distribution of cantilever structure subject to static load, b) corresponding points in a two-dimensional LSF space, where s_{i1}, s_{i2} are normalized elemental strain energy and density, respectively, with clusters by choosing 4 prototype elements, and c) resulting groups of elements in the design space.

on the objective function, i.e. elements that are close to each other in LSF space. By choosing a user defined characteristic LSF vector, a lower dimensional representation based on the structural state is defined. Then, groups of elements with similar LSF can be represented by one optimization variable each.

Concretely, we propose to apply a simple form of vector quantization: The data set $\mathcal{V}$ is mapped to a finite set of indices, obtained from L randomly chosen prototype elements. The corresponding LSF vectors $\mathbf{c}_l \in \mathcal{V},\ l \in \{1,\dots,L\}$ of the prototypes define clusters in LSF space. A mapping Ψ can be defined that maps each sample in data set $\mathcal{V}$ to an index, as:

$$\Psi_{\mathcal{V}\to\{1,\dots,L\}} : \mathbf{s}_i \to \zeta_i = \arg \min_{l\in\{1,\dots,L\}} (\text{dist}(\mathbf{s}_i, \mathbf{c}_l)) \qquad (3)$$

with the Euclidean distance metric $\text{dist}(\mathbf{s}_i, \mathbf{c}_l)$. Thus, each sample in $\mathcal{V}$ is assigned to a cluster with index $\zeta_i = \Psi(\mathbf{s}_i)$.

This relates to a subdivision of the LSF space in Voronoi cells. In contrast to existing work [11] the Voronoi cells are defined in LSF space and not in the Cartesian coordinates of the design space. An example for the resulting clusters in LSF space and the corresponding elements in the design space is shown in Fig. 3b) and c), respectively. With the random prototypes each point in LSF space is assigned to one cluster of LSF points, highlighted by different colors in the figure. The elements represented by the clusters of LSF vectors can be mapped back to the design space, where they are not necessarily connected.

The number of prototypes can be chosen by the user, depending on the desired precision of the quantization. In the limit case $L \to N$, in which the number of prototypes approaches the total number of elements, each element becomes a prototype. An advantage is that L is decoupled from N, thus preferably $L << N$ is chosen. Hence, it is conceptually possible to address design spaces, where for instance $N \sim 10^6$. This is computationally infeasible for naive approaches that apply a direct bit array representation with one variable per element, since the search space dimensionality is critical in terms of performance and cost of an evolutionary search.

The prototypes represent the structure depending on its state. By assigning an individual optimization variable to each prototype, a vector $\boldsymbol{\theta} = [\theta_1 \dots \theta_L]^T \in \mathbb{R}^L$ of search variables for the evolutionary optimization is obtained.

III. Optimization Method

This section presents an optimization method for the state-based representation introduced in the preceding section. Since the proposed representation of the structure is based on the state, which is a function of the material distribution, i.e. $\mathbf{u} = \mathbf{u}(\boldsymbol{\rho})$, any change in the structure will result in a change of the state. The new state leads to different cluster assignments of the elements and eventually it is necessary to determine new prototypes that account for the change and reduce the quantization error. Therefore, it makes sense to only change the structure gradually. We propose that the vector of optimization variables $\boldsymbol{\theta}$ does not encode the material, but instead an update signal vector $[\theta_{\zeta_1}, \dots, \theta_{\zeta_i}, \dots, \theta_{\zeta_N}]^T$, that determines the *change* of the material.

Concretely, an update signal is assigned to each element prototype and its cluster of elements, resulting in a piecewise constant function in LSF space. When this function is mapped back to the design space, it can be used to determine the increase or decrease of the density in the corresponding elements. An example illustrating the idea is shown in the experiments section in Fig. 6.

The update signal vector is in fact analogue to modeling parameter sensitivities i.e. partial derivatives used by gradient-based methods: $\theta_{\zeta_i} \sim \frac{\partial f}{\partial \rho_i}$. From this perspective the update signal is a generic model for the sensitivity based on the structural state. Since it is composed of local zero-order models we designate the approach Topology Optimization by Predicting Sensitivities with Piecewise Constant Model (PCM-TOPS).

Consequently, an efficient update scheme from the field of gradient-based topology optimization can be used. The Optimality Criteria (OC) update [1] obtains an updated structure $\boldsymbol{\rho}_i^{\text{new}} = [\rho_1^{\text{new}} \dots\ \rho_i^{\text{new}} \dots\ \rho_N^{\text{new}}]^T$ according to:

$$\rho_i^{\text{new}}(\theta_{\zeta_i}) = \begin{cases} \max(\rho_{\texttt{min}}, \rho_i - m) \\ \quad \text{if } \rho_i B_i^\eta \le \max(\rho_{\min}, \rho_i - m), \\ \min(1, \rho_i + m) \\ \quad \text{if } \min(1, \rho_i + m) \le \rho_i B_i^\eta, \\ \rho_i B_i^\eta \text{ else } , \end{cases} \qquad (4)$$

where m is a move limit, and η is a damping parameter controlling the amount of change that occurs during one update. Typical values are $m = 0.1$ and $\eta = 0.5$. Here, $B = \min(0, \theta_{\zeta_i(\mathbf{s}_i)})/\Lambda$ is depending on the update signal and a multiplier Λ. The OC scheme is an intuitive heuristic update scheme, that increases the density in elements with low update signal and decreases the density in elements with a high update signal (assuming minimization). It does so while maintaining

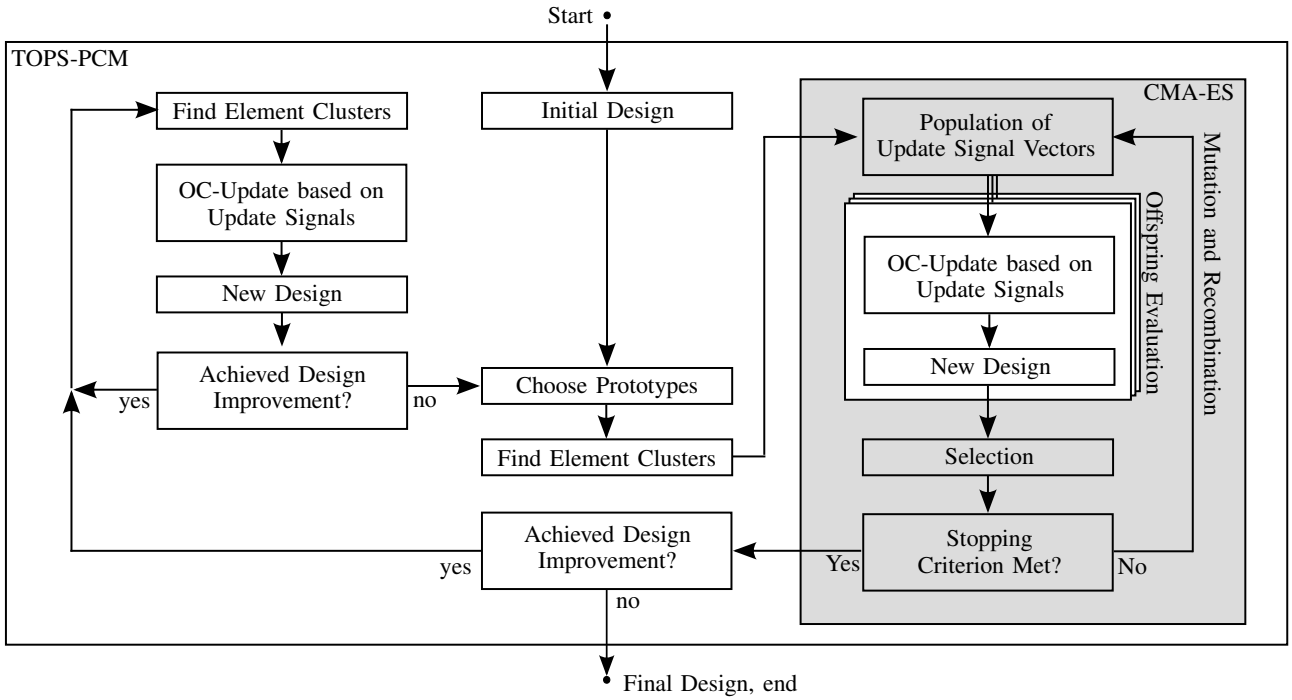

Fig. 4. The computational flow for PCM-TOPS approach.

the volume constraint G_0 by adjusting Λ, by a bi-sectioning algorithm. Since the OC-update can only deal with negative input values, values larger than zero of the update signal are cut.

In order to avoid numerical instabilities and in order to impose a minimum length scale, the update signal is spatially filtered with radius $r_{\min}$ according to a sensitivity filtering approach [19], which is a popular technique in the field of topology optimization. For details on the issue of regularization in topology optimization the reader is referred to [1], [20].

A standard evolutionary optimizer can be applied to tune the update signals. Since the vector of update signals is continuous it makes sense to apply an evolutionary search strategy. The Covariance Matrix Adaptation Evolutionary Strategy (CMA-ES) [21], [22] is one of the best currently existing stochastic optimization methods for real-valued problems. It is a derandomized version of evolution strategies, that utilizes the information collected by successful mutations in the previous iterations to estimate the mutation covariance matrix. It is especially useful for computationally expensive industrial optimization problems, since it finds improved solutions with a relatively low number of evaluations [23].

The computational flow of PCM-TOPS is shown in Fig. 4. Overall, two optimization loops can be distinguished. The outer loop is the actual topology optimization addressing problem (1). It effectively is a density-based topology optimization as in [1], [24] yet based on the generic update signals instead of sensitivities. The algorithm is started with an initial design guess (e.g. a homogenous distribution of material). Then the first prototypes are determined and the elements are assigned to the respective clusters. For initially optimizing the update signal the CMA-ES inner loop is started. The fitness of an update signal is defined as the objective of the structure used in the outer topology optimization loop, after performing a design update based on (4). Thus, the fitness is computed by emulating a single topology optimization update step, i.e. the CMA-ES minimizes:

$$\min_{\boldsymbol{\theta}} f(\boldsymbol{\rho}^{\mathrm{new}}) \ . \tag{5}$$

In the subsequent step, it is checked if the design improved based on the optimized update signals. This is achieved by a check of the actual progress and a consequent branch, a basic version of the scheme in [18]. Concretely, the relative design improvement Δf_{rel} is measured as:

$$\Delta f_{\mathrm{rel}} = (f^{(\mathrm{k})} - f^{(\mathrm{k}+1)})/f^{(\mathrm{k})} \ . \tag{6}$$

In case $\Delta f_{\mathrm{rel}} > \Delta f_{\min}$, with a minimum improvement threshold $\Delta f_{\min}$, the optimized update signals are used to modify the structure. Since it would be computationally expensive to optimize the update signals every iteration, the improvement threshold is checked again after the design update. As long as this is fulfilled, the optimized update signal vector is reused. This avoids to run more CMA-ES optimizations, than actually necessary to achieve improvement of the structure.

The improvement threshold may not be fulfilled either because the structure is converged, or because new update signals are required. Assuming the second possibility, new prototypes are determined based on the changed structural state and the CMA-ES optimization is performed again. By defining new

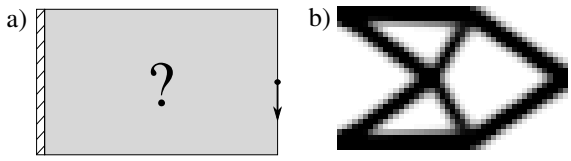

Fig. 5. Example for a) design space and boundary conditions of a cantilever topology optimization problem and b) optimized design [24].

Setting	Symbol	Value
Young's modulus	E_0	1MPa
Poisson's ratio	ν	0.3
Number of prototypes	L	150
Penalization	p	3
Parents	μ	9
Offspring	λ	19
Max. evaluations	-	3000
CMA-ES initial global step size	σ_{init}	0.3
Min. improvement threshold	$\Delta f_{\min}$	0.001
Filter radius	$r_{\min}$	2mm

TABLE I
PCM-TOPS SPECIFICATIONS FOR COMPLIANCE CANTILEVER OPTIMIZATION.

prototypes, an adaptation of the representation is realized, as reaction to the changed material distribution. The adaptation achieves that the quantization error induced by the clustering is kept low, facilitating a low number of prototypes and hence a feasible dimensionality for the evolutionary search. If the updated structure is not achieving the improvement threshold after the CMA-ES optimization was performed, the structure is considered converged and the overall optimization is stopped.

IV. EXPERIMENTS

A. Cantilever Compliance Minimization

PCM-TOPS is at first validated on the reference problem of maximizing the stiffness, i.e. minimizing the compliance of a cantilever. The design space with loads and supports is shown in Fig. 5a).

The problem in its finite element form can be stated as:

$$\begin{aligned} \min_{\boldsymbol{\rho}} c(\boldsymbol{\rho}) &= \mathbf{u}^T\mathbf{l} \\ \text{s.t. : } & \sum_{i=1}^{N}(\rho_i^p\mathbf{K}_i)\mathbf{u} = \mathbf{l}, \\ & V(\boldsymbol{\rho})/V_0 = 0.4, \\ & 0.001 \le \rho_i \le 1,\ i = 1,\dots,N\ . \end{aligned} \tag{7}$$

The objective function $c(\boldsymbol{\rho})$ is the compliance of the structure. Here, $\mathbf{l}$ is the load vector, and the governing equation is the linear static state equation. The global stiffness matrix is constructed by superposing elemental stiffness matrices $\mathbf{K}_i(\rho_i)$ (see [24]), in which the Young's modulus is replaced according to the SIMP interpolation (2) and thus the stiffness matrix is a function of the elemental densities. The design space is meshed with 45×28 plane finite elements with 1mm edge length. The reference solution in Fig. 5b) is obtained by a gradient-based approach [24].

Important for the approach is the choice of LSF vectors $\mathbf{s}_i$ on which the representation is based. We consider two experiments with different LSF vectors, I and II:

$$\mathbf{s}_i^{\text{I}} = (\rho_i\ \text{SED}_i)^{\text{T}},\ \mathbf{s}_i^{\text{II}} = (\rho_i\ u_{i1}\ \dots\ u_{i8})^{\text{T}}\ , \tag{8}$$

with the elemental strain energy density SED_i and the nodal displacements $u_{ij},\ j = 1,\dots,8$ as in Fig. 2. LSF Vector I $\mathbf{s}_i^{\text{I}}$ contains the elemental strain energy density as LSF. This enables to cluster all elements with similar energy density and hence material can be added and removed accordingly, similar to gradient-based topology optimization methods. By using the nodal displacements, LSF Vector II $\mathbf{s}_i^{\text{II}}$ contains energy information implicitly, yet in more primitive form. Before applying the clustering, all LSF vector components are normalized to zero mean and unit standard deviation. Table I shows the parameter settings. A public implementation of the CMA-ES[1] [22] is used and it is stopped after a maximum number of evaluations. The finite element solver from [24] is used for the analysis.

Figure 6 illustrates the update signal vector optimized in the first iteration of the best run of the experiments with LSF Vector II. For application of the OC-update (4), the update signals are cut if larger than zero, which is also done in the plots in Fig. 6b) and c). Fig. 6c) shows most areas where the density will be reduced in dark blue. It can be seen that already in the first iteration, the update signal differentiates regions similar to those of the reference structure.

Figure 7 shows the final objective and the total number of evaluations of 30 runs. This is complemented by Fig. 8 showing the development of the compliance with respect to the evaluations.

There is a significant difference between the two LSF vectors. For problem (7) the strain energy density effectively is gradient information. For LSF Vector I, when the strain energy density is used, a solution with lower compliance than the reference is found after about $6,000$ evaluations. The update signal that is optimized by the CMA-ES in the first iteration is reused several times, visible by the vertical descent of the compliance. Towards the end of the optimization the solution is improved marginally by continued optimization of the update signal. Using the strain energy density as LSF results in such a fast optimization, since the model enables the easy separation in elements with large and low strain energy density and the according increase and decrease in material. The result is also reflected in the optimized structures that visually strongly resemble the reference, see Fig. 9. Also for LSF Vector II, the resulting structures are very similar to the reference. The compliance is approaching the reference. Since the higher dimensional LSF vector based on displacements requires a longer and more frequent optimization of the update signal, only in some iterations it is reused.

By reproduction of the reference, the feasibility of PCM-TOPS is demonstrated. The difference between the two LSF vectors additionally highlights the ability of PCM-TOPS to

[1]Source from: https://www.lri.fr/~hansen/cmaes_inmatlab.html

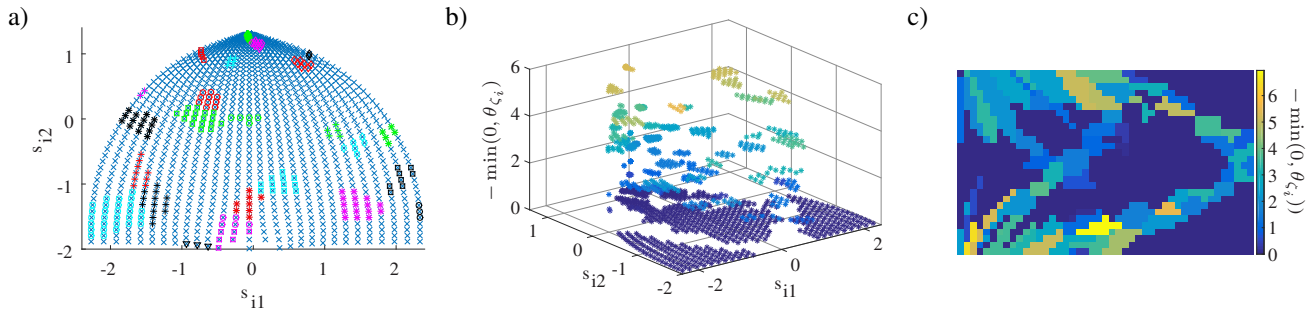

Fig. 6. Example illustration of LSF space and update signals: a) Points in LSF space spanned by the first two components of the LSF vector, highlighting 25 of 150 clusters; b) Presentation of the optimized piecewise constant update signal added as a third dimension orthogonally to the LSF space from a); c) Presentation of the update signal from b) mapped back to the design space. For the presented plots, values larger zero of the update signal are cut and the result is inverted.

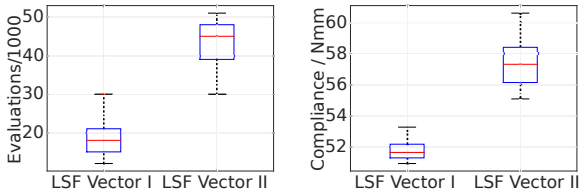

Fig. 7. Optimized compliance values (left) and required evaluations (right).

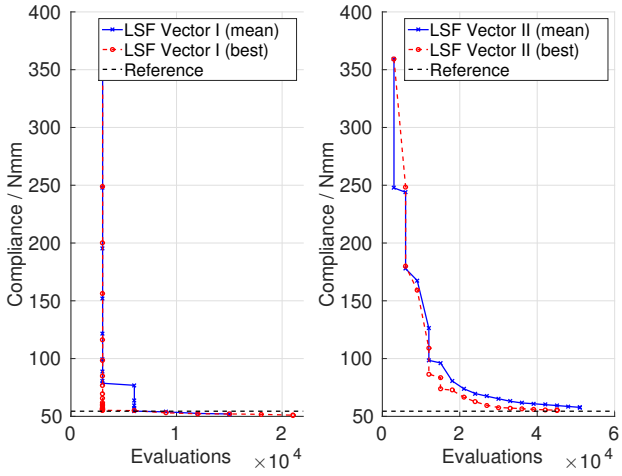

Fig. 8. The compliance of the mean and best run versus the number of function evaluations.

systematically utilize gradients or gradient approximations and accordingly the potential for increasing computational efficiency, which does not exist in the majority of other evolutionary computation approaches for topology optimization.

B. Frame Crash Intrusion Minimization

In this section, a practically relevant problem from the automotive industry is considered. In many vehicle crash scenarios, minimal or at least constraint displacements are desired at selected locations in order to protect other components or areas from deformation. The considered crash case is inspired by the side pole impact of the Euro NCAP crash test [25], in which a vehicle is moving laterally into a pole like structure with high

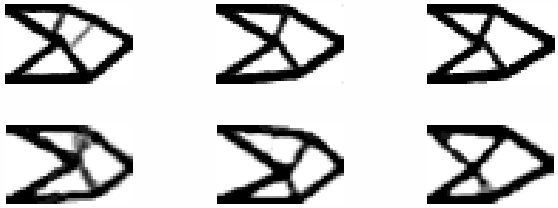

Fig. 9. Optimized structures obtained for LSF Vector I (top row) and LSF Vector II (bottom row), from left to right: worst run, mean run and the best run.

risk of injuries of the passengers.

We consider a simulation model of a 3-dimensional aluminum frame supported at both ends, meshed with $15 \times 100 \times 4 = 6,000$ shell elements with 4mm edge length that is crashed with a rigid pole with initial velocity of 30km/h. A piecewise linear elastic-plastic aluminum material model is used with material parameters as in literature [26]. The frame is shown in Fig. 10.

The considered optimization problem is formulated as:

$$\begin{aligned} \min_{\boldsymbol{\rho}} \mathrm{I}(\boldsymbol{\rho}) &= \frac{1}{196} \sum_{i \in \mathcal{N}_\mathrm{I}} (\min_t u_{zi}(t))^2 \\ \text{s.t.} : \mathbf{r}(t, \boldsymbol{\rho}, \mathbf{u}) &= \mathbf{0}, \\ V(\boldsymbol{\rho})/V_0 &= 0.2, \\ 0.1 \leq \rho_i \leq 1,\ i &= 1, \ldots, N\ , \end{aligned} \tag{9}$$

with time step t, nodal displacement $u_{zi}(t)$ in z-direction, a set of node indices $\mathcal{N}_\mathrm{I}$ and the intrusion measure $\mathrm{I}(\boldsymbol{\rho})$. Figure 10b) highlights the area in which the indices of the nodes belong to $\mathcal{N}_\mathrm{I}$. The intrusion is quantified by the squared maximum of the displacement of the nodes within a rectangular area at the center of the bottom side of the frame, consisting of 196 nodes. We explicitly target intrusion at a defined location, that differs to the location of the impact. The state equation is represented by the residual of the dynamic finite element analysis $\mathbf{r}(t, \boldsymbol{\rho}, \mathbf{u})$. Here, the design variables ρ_i refer to the thickness of the elements scaled by a factor of ten.

The state of an element is reflected by the amount of elastic and plastic deformation, hence we chose the maximum of the internal energy density $\mathrm{IED}_i(t)$ absorbed by an element as

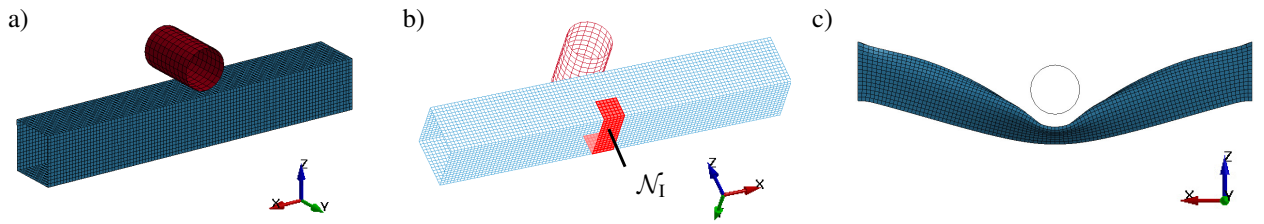

Fig. 10. The frame structure subject to the impact of a rigid pole: frame and pole (a), node group $\mathcal{N}_\mathrm{I}$ relating to the objective function (b), initial uniform thickness structure at the end of the crash simulation (c).

	Symbol	Value
Pole mass	-	100kg
Frame mass	-	2.5kg
Young's modulus	E_0	$70,000$MPa
Mass density	ϱ_0	$2.7 \cdot 10^{-9}$t/mm^3
Poisson's ratio	ν	0.33
Yield stress	σ_{y0}	180MPa
Number of prototypes	L	15
Filter radius	r_min	6.0mm
Parents	μ	6
Offpring	λ	12
Max. evaluations	-	600
Initial global step size	σ_init	0.3
Min. improvement threshold	Δf_min	0.001

TABLE II
PCM-TOPS SPECIFICATIONS FOR FRAME CRASH OPTIMIZATION.

LSF, resulting in the LSF vector:

$$\mathbf{s}_i = \left(\rho_i, \max_t(\mathrm{IED}_i(t))\right)^\mathrm{T} . \tag{10}$$

For the considered problem, precise mathematical gradients are not available. Instead, as baseline for comparison, the Hybrid Cellular Automata (HCA) algorithm for crashworthiness topology optimization [4] is used, as one of few existing and practically applied heuristics. Instead of applying gradients, it targets an uniform energy distribution throughout the structure, assuming that the best structure is obtained when all of its elements absorb the same amount of energy. The HCA implementation provided by the tool LS-TaSC [27] is used with default parameters. It is an efficient heuristic to optimize, for instance, objective functions with respect to compliance or energy absorbing structures [4], [26], yet the fixed heuristic scheme does not permit to explicitly account for changed objective functions. This fact justifies the usage of PCM-TOPS for the considered crash problem. Although a large statistical basis is desired for evaluation of this stochastic approach, the available computational time permitted only three runs with different random seeds. The parameter choices and model details are shown in Tab. II.

The optimized thickness distribution obtained by the best PCM-TOPS run is shown in Fig. 11a). The areas along the top edges of the frame are increased in thickness, especially close to the supports. The lower side of the frame is driven to the minimum thickness. Near the impact, the structure is as well reinforced. In the three tested runs, new update signals

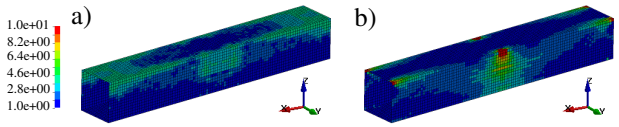

Fig. 11. Optimized frames of PCM-TOPS (a) and of HCA (b), color coded by the elemental thickness in mm.

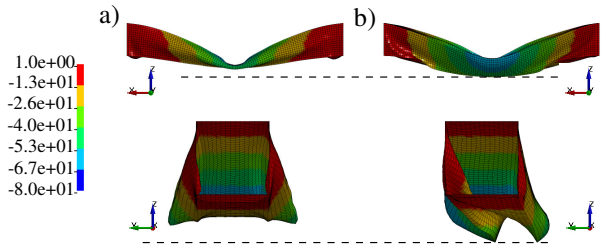

Fig. 12. Optimized frames of PCM-TOPS (a) and of HCA (b), color coded by the deformation in z-direction at the final simulation time step in mm.

are optimized in most iterations, in average resulting in a total of $4,400$ evaluations during nine iterations.

The HCA baseline algorithm was stopped after 100 iterations (and 100 evaluations accordingly) when the algorithm specific mass redistribution convergence criterion was clearly oscillating periodically. A quite different structure is obtained, that can be seen in Fig. 11b).

The deformation of the PCM-TOPS structure and the HCA baseline structure is shown in Fig. 12. It is clearly visible that the deformation in the vertical direction is smaller for the structure obtained by the state-based representation approach.

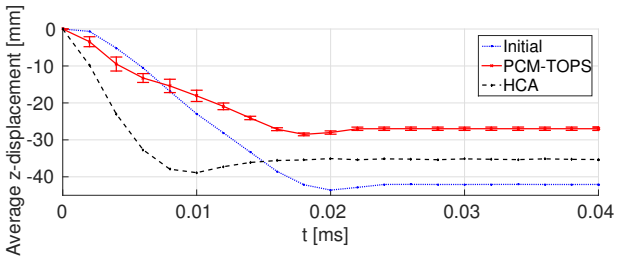

Fig. 13. The average z-displacement $\overline{u}_z(t)$ of the intruding node set $\mathcal{N}_\mathrm{I}$ during the crash event, for the initial and the optimized designs by PCM-TOPS and HCA.

Also, the deformation is very uniform and flat in the area of the intrusion node set. The optimization with HCA results in much larger deformations. The smoothness of the resulting deformations might be interesting as well, since from a safety perspective it is favorable to avoid sharp edges that bear potential risk for injuries.

Figure 13 shows the average z-displacement of the node set $\overline{u}_z(t) = \frac{1}{196}\sum_{i\in\mathcal{N}_\mathrm{I}} u_{zi}(t)$. The result from PCM-TOPS has significantly lower average displacement for most simulation time steps, compared to the initial uniform thickness structure, as well as compared to the HCA result.

Overall, the PCM-TOPS approach achieves a remarkably lower intrusion measure compared to the HCA. The most likely reason is that the fundamental assumption of a uniform energy distribution is not applicable for the given objective function and there is no concept for appropriate adaptation. This underlines the systematic advantage of the generic PCM-TOPS approach compared to a specialized heuristic.

V. Conclusion

This paper introduces a novel evolutionary approach for the industrial problem of topology optimization of mechanical structures. Proposed is a state-based representation, utilizing optimized update signals that determine the increase or decrease of material throughout the design space. First the feasibility of the approach is demonstrated on the minimum compliance problem by reproduction of reference structures. Lowest compliance results are obtained when the strain energy density is included as Local State Feature. With an increased number of evaluations, also for basic displacement features, reproductions of the reference are obtained. Subsequently, the approach is applied to a frame crash problem. It achieves a remarkably lower intrusion compared to a baseline obtained by an heuristic uniform energy approach.

References

[1] M. Bendsøe and O. Sigmund, *Topology Optimization Theory, Methods and Applications*, 2nd ed. Springer Verlag Berlin, 2004.

[2] O. Sigmund and K. Maute, "Topology optimization approaches," *Structural and Multidisciplinary Optimization*, vol. 48, no. 6, pp. 1031–1055, 2013.

[3] M. Bendsøe, "Optimal shape design as a material distribution problem," *Structural optimization*, vol. 1, pp. 193–202, 1989.

[4] N. M. Patel, B.-S. Kang, J. E. Renaud, and A. Tovar, "Crashworthiness design using topology optimization," *Journal of Mechanical Design*, vol. 131, p. 061013, 2009.

[5] C. Ortmann and A. Schumacher, "Graph and heuristic based topology optimization of crash loaded structures," *Structural and Multidisciplinary Optimization*, vol. 47, no. 6, pp. 839–854, 2013.

[6] R. Kicinger, T. Arciszewski, and K. De Jong, "Evolutionary computation and structural design: A survey of the state-of-the-art," *Computers & Structures*, vol. 83, no. 23, pp. 1943–1978, 2005.

[7] N. Aulig and M. Olhofer, "Evolutionary computation for topology optimization of mechanical structures: An overview of representations," in *Proceedings of: IEEE Congress on Evolutionary Computation (accepted)*, Vancouver, BC, Canada, 2016.

[8] R. Balamurugan, C. Ramakrishnan, and N. Swaminathan, "A two phase approach based on skeleton convergence and geometric variables for topology optimization using genetic algorithm," *Structural and Multidisciplinary Optimization*, vol. 43, no. 3, pp. 381–404, 2011.

[9] D. Sharma, K. Deb, and N. Kishore, "Domain-specific initial population strategy for compliant mechanisms using customized genetic algorithm," *Structural and Multidisciplinary Optimization*, vol. 43, no. 4, pp. 541–554, 2011.

[10] O. Sigmund, "On the usefulness of non-gradient approaches in topology optimization," *Structural and Multidisciplinary Optimization*, vol. 43, pp. 589–596, 2011.

[11] M. Schoenauer, "Shape representations and evolution schemes." *Evolutionary Programming*, vol. 5, 1996.

[12] F. Ahmed, B. Bhattacharya, and K. Deb, "Constructive solid geometry based topology optimization using evolutionary algorithm," in *Proceedings of Seventh International Conference on Bio-Inspired Computing: Theories and Applications (BIC-TA 2012)*, ser. Advances in Intelligent Systems and Computing, J. C. Bansal, P. K. Singh, K. Deep, M. Pant, and A. K. Nagar, Eds. Springer India, 2013, vol. 201, pp. 227–238.

[13] C. Jain and A. Saxena, "An improved material-mask overlay strategy for topology optimization of structures and compliant mechanisms," *Journal of Mechanical Design*, vol. 132, no. 6, p. 061006, 2010.

[14] T. Steiner, Y. Jin, and B. Sendhoff, "A cellular model for the evolutionary development of lightweight material with an inner structure," in *Proceedings of the Genetic and Evolutionary Computation Conference (GECCO 2008)*. New York, NY, USA: ACM, 2008.

[15] H.-T. C. Pedro and M. H. Kobayashi, "On a cellular division method for topology optimization," *International Journal for Numerical Methods in Engineering*, vol. 88, no. 11, pp. 1175–1197, 2011.

[16] N. Cheney, E. Ritz, and H. Lipson, "Automated vibrational design and natural frequency tuning of multi-material structures," in *Proceedings of the 2014 Conference on Genetic and Evolutionary Computation*, ser. GECCO '14. New York, NY, USA: ACM, 2014, pp. 1079–1086.

[17] N. Aulig and M. Olhofer, "Neuro-evolutionary topology optimization of structures by utilizing local state features," in *Proceedings of the 2014 Conference on Genetic and Evolutionary Computation*, ser. GECCO '14. New York, NY, USA: ACM, 2014, pp. 967–974.

[18] N. Aulig and M. Olhofer, "Neuro-evolutionary topology optimization with adaptive improvement threshold," in *Applications of Evolutionary Computation*, ser. Lecture Notes in Computer Science. Springer International Publishing, 2015, vol. 9028, pp. 655–666.

[19] J. Sigmund, O.; Petersson, "Numerical instabilities in topology optimization: a survey on procedures dealing with checkerboards, mesh-dependencies and local minima," *Struct. Optim.*, vol. 16, pp. 68–75, 1998.

[20] O. Sigmund, "Morphology-based black and white filters for topology optimization," *Structural and Multidisciplinary Optimization*, vol. 33, no. 4-5, pp. 401–424, 2007.

[21] N. Hansen and A. Ostermeier, "Completely derandomized self-adaptation in evolution strategies," *Evolutionary Computation*, vol. 9, no. 2, pp. 159–195, 2001.

[22] N. Hansen, "The CMA evolution strategy: A comparing review," in *Towards a New Evolutionary Computation*, ser. Studies in Fuzziness and Soft Computing, J. Lozano, P. Larrañaga, I. Inza, and E. Bengoetxea, Eds. Springer Berlin Heidelberg, 2006, vol. 192, pp. 75–102.

[23] T. Bäck, C. Foussette, and P. Krause, *Contemporarey Evolution Strategies*, ser. 1619-7127. Springer Verlag Berlin Heidelberg, 2013.

[24] E. Andreassen, A. Clausen, M. Schevenels, B. Lazarov, and O. Sigmund, "Efficient topology optimization in matlab using 88 lines of code," *Structural and Multidisciplinary Optimization*, vol. 43, no. 1, pp. 1–16, 2011.

[25] European New Car Assessment Programme (Euro NCAP), "Oblique pole side impact testing protocol version 7.0.2," November 2015. [Online]. Available: http://www.euroncap.com/de/fuer-ingenieure/protocols/adult-occupant-protection/

[26] N. Aulig, S. Menzel, E. Nutwell, and D. Detwiler, "Towards multi-objective topology optimization of structures subject to crash and static load cases," in *International conference on Engineering Optimization (Engopt 2014)*. Portugal: CRC Press, September 2014, pp. 847–852.

[27] W. Roux, "Topology design using LS-TaSC^{TM} version 2 and LS-DYNA," in *8th European LS-DYNA Users Conference*, 2011.